Journal of Magnetic Resonance 206 (2010) 134–138

Contents lists available at ScienceDirect

Journal of Magnetic Resonance

journal homepage: www.elsevier.com/locate/jmr

hnCOcaNH and hncoCANH pulse sequences for rapid and unambiguous backbone assignment in (^{13}C, ^{15}N) labeled proteins

Dinesh Kumar [a], Jithender G. Reddy [a], Ramakrishna V. Hosur [a,b,*]

[a] Department of Chemical Sciences, Tata Institute of Fundamental Research (TIFR), 1-Homi Bhabha Road, Colaba, Mumbai 400 005, India
[b] UM-DAE Centre for Excellence in Basic Sciences, Mumbai University Campus, Kalina, Santa Cruz, Mumbai 400 098, India

ARTICLE INFO

Article history:
Received 9 May 2010
Available online 30 June 2010

Keywords:
Multidimensional NMR
Backbone assignment
Sequential correlation
hncoCANH
hnCOcaNH
Check points

ABSTRACT

Time-saving in data acquisition is a major thrust of NMR pulse sequence development in the context of structural proteomics research. The conventional HNCA and HN(CA)CO pulse sequences, routinely used for sequential backbone assignment, have the limitation that they cannot distinguish inter- and intra-residue correlations. In order to remove this ambiguity, one has to record HNCO and HN(CO)CA or sequential HNCA experiments which provide unambiguous information of sequential correlations. However, this almost doubles the experimental time. Besides, they require repeated scanning through the ^{15}N planes to search for the matching peaks along the carbon dimension. In this background, we present here two pulse sequences, termed as hncoCANH and hnCOcaNH that lead to spectra equivalent to HNCA and HN(CA)CO spectra, respectively, but with direct distinction of inter- and intra-residue peaks; these occur with opposite signs in the new experiments. The two pulse sequences have been derived by simple modification of the previously described HN(C)N pulse sequence [Panchal et al., J. Biomol. NMR 20 (2001) 135–147] to frequency-label $^{13}C^{\alpha}$ or $^{13}C'$ instead of ^{15}N during the t_1 period. Like HN(C)N, these spectra also exhibit special patterns of self and sequential peaks around glycines and prolines, which enable direct identification of certain triplets of residues and thus provide internal checks during the sequential assignment walk. The spectra enable rapid and unambiguous assignment of H^N, ^{15}N and $^{13}C^{\alpha}$ (or $^{13}C'$) in a single experiment, and thus would be of great value in high-throughput structural proteomics.

1. Introduction

In the present post-genomic era, the structural and functional proteomics has occupied the center stage of NMR research. The primary requirement for all investigations of proteins by NMR is the sequence specific resonance assignment, and a number of experiments have been proposed for getting sequence specific assignments (reviewed here [1]). However, in the context of high-throughput NMR for structural and functional proteomics research the currently used standard multidimensional NMR experiments are highly time consuming in terms of data acquisition. For example, CBCANH [2]/HNCACB [3], HNCA [4,5], and HN(CA)CO [6] which are used to obtain $^{1}H^{N}$, ^{15}N, $^{13}C^{\alpha}$, $^{13}C^{\beta}$ and $^{13}C'$ assignments suffer from the fact that each experiment needs a complementary one (CBCACONH [7], sequential HNCA [8]/HN(CO)CA [4]/intra-HNCA [9] and HNCO [4,5])/intra-HN(CA)CO [10] for making distinction between self and sequential correlations. This in turn increases the demand for NMR experimental time. This also imposes a condition of long term stability on the protein samples. Additionally, some proteins in solution tend to precipitate in matter of days, thereby reducing the time available to record NMR data. Besides, the standard experiments require repeated scanning through the ^{15}N planes of the 3D spectra to search for the matching peaks along the Carbon dimension. In this background, we present here two novel pulse sequences – hncoCANH and hnCOcaNH – for rapid sequential backbone assignment of $^{1}H^{N}$, ^{15}N, $^{13}C^{\alpha}$ and $^{13}C'$ resonances of proteins; the experiments proposed here lead to spectra where the inter- and intra-residue correlation peaks can be easily identified by their opposite signs. These new pulse sequences (Fig. 1) are a result of an extremely simple modification of the previously described HN(C)N pulse sequence [11]. They differ from basic HN(C)N pulse sequence only in terms of t_1 evolution; this involves here evolution of ^{13}C magnetization rather than of ^{15}N magnetization. However like HN(C)N, these spectra also exhibit special patterns of self and sequential peaks that arise around glycines and prolines. These special patterns enable direct identification of certain triplets of residues and hence provide internal

Abbreviations: NMR, nuclear magnetic resonance; HSQC, heteronuclear single quantum correlation; TE, transfer efficiency.

* Corresponding author. Address: Department of Chemical Sciences, Tata Institute of Fundamental Research (TIFR), 1-Homi Bhabha Road, Colaba, Mumbai 400 005, India. Fax: +91 22 22804610.
E-mail address: hosur@tifr.res.in (R.V. Hosur).

1090-7807/$ - see front matter © 2010 Elsevier Inc. All rights reserved.
doi:10.1016/j.jmr.2010.06.013

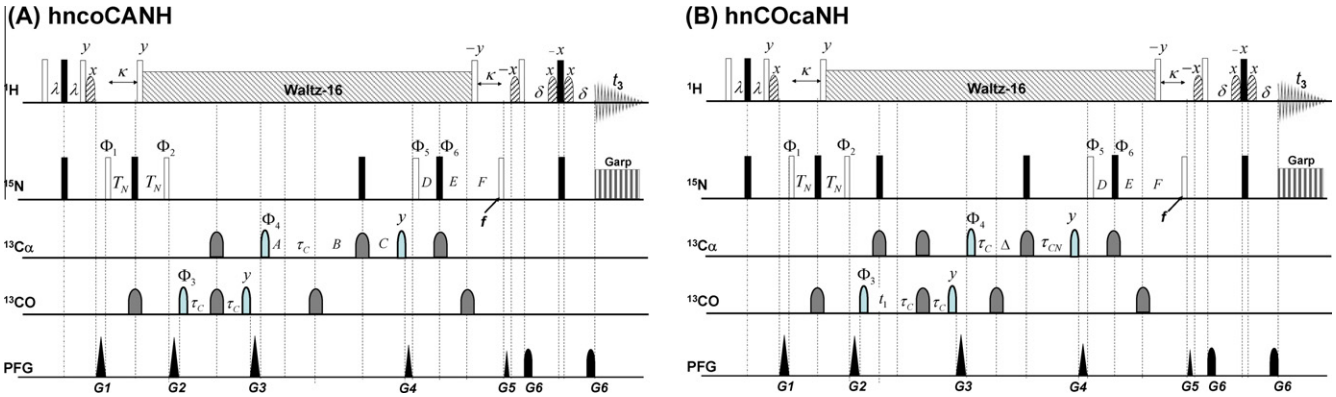

Fig. 1. Pulse sequences for: (A) hncoCANH and (B) hnCOcaNH experiments. Narrow (hollow) and wide (filled black) rectangular bars represent non-selective 90° and 180° pulse, respectively. Unless indicated, the pulses are applied with phase *x*. The ^{1}H and ^{15}N carrier frequencies are set at 4.7 ppm (water) and 119.0 ppm, respectively. The ^{13}C carrier frequency respectively for pulses in $^{13}C^{\alpha}$ and $^{13}C'$ channel are set at 54.0 ppm and 172.5 ppm. Proton decoupling using the waltz-16 decoupling sequence [15,16] with field strength of 6.3 kHz is applied during most of the t_1 and t_2 evolution periods, and ^{15}N decoupling using the GARP-1 sequence [17] with the field strength 0.9 kHz is applied during acquisition. The strength of the $^{13}C^{\alpha}$ pulses (standard Gaussian cascade Q3 (180°) and Q5 (90°) pulses) [13] is adjusted so that they cause minimal excitation of carbonyl carbons. The 180° $^{13}C'$ shaped pulse (width 200 μs) had a standard Gaussian cascade Q3 pulse profile with minimal excitation of $^{13}C^{\alpha}$. The values for the individual periods containing t_1 (in hncoCANH experiment) are: $A = t_1/2$, $B = \tau_{CN} - \tau_C$, and $C = \tau_{CN} - t_1/2$. The values for the individual periods containing t_2 in both the experiments are: $D = \tau_N - t_2/2$, $E = \tau_N$, and $F = t_2/2$. The delays are set to $\lambda = 2.7$ ms, $\kappa = 5.4$ ms, $\delta = 2.7$ ms, $\tau_C = 4.5$ ms, $T_N = 14$ ms, $\tau_{CN} = 12.5$ ms, $\Delta = \tau_{CN} - \tau_C$, and $\tau_N = 15$ ms. The τ_{CN} must be optimized and are around 12–15 ms. The phase cycling for the experiment is $\Phi_1 = 2(x), 2(-x)$; $\Phi_2 = \Phi_3 = x, -x$; $\Phi_4 = \Phi_5 = x$; $\Phi_6 = 4(x), 4(-x)$; and $\Phi_{receiver} = 2(x), 4(-x), 2(x)$. In hncoCANH experiment frequency discrimination in t_1 and t_2 has been achieved using States-TPPI phase cycling [18] of Φ_4 and Φ_5, respectively, along with the receiver phase. In hnCOcaNH experiment frequency discrimination in t_1 and t_2 has been achieved using States-TPPI phase cycling [18] of Φ_3 and Φ_5, respectively, along with the receiver phase. The gradient (sine-bell shaped; 1 ms) levels are as follows: $G_1 = 30\%$, $G_2 = 30\%$, $G_3 = 30\%$, $G_4 = 30\%$, $G_5 = 50\%$, and $G_6 = 80\%$ of the maximum strength 53 G/cm in the z-direction. The recovery time after each gradient pulse was 160 μs. Before detection, WATERGATE sequence [19] has been employed for better water suppression.

checks for the sequential assignment procedure. We anticipate that the experiments described here can be of immense value for research in protein NMR.

2. Materials and methods

The 3D-hncoCANH and 3D-hnCOcaNH pulse sequences (Fig. 1) were tested on 1.6 mM uniformly $^{15}N/^{13}C$ labeled human ubiquitin dissolved in phosphate buffer pH 6.5 in 90% H_2O and 10% D_2O (a product from Cambridge Isotope Laboratories, Inc.). All NMR experiments were performed at 25 °C on a Bruker Avance III spectrometer equipped with a cryoprobe, operating at ^{1}H frequency of 800 MHz. The delays $2T_N$, $2\tau_C$, $2\tau_{CN}$, and $2\tau_N$ were set to 28, 9, 25, and 30 ms, respectively. For each 3D experiment, 1024 complex points were collected along the direct dimension while 32 complex points were used along both the indirect dimensions. For each increment, 16 scans were accumulated. The recycling delay was set to 0.7 s for both the experiments. The acquisition time in each case was approximately 16 h 10 min. All the spectra were processed using Topspin (BRUKER, http://www.bruker.com/) and analyzed using CARA [12]. Gaussian cascade Q5 and Q3 pulses [13] were used for band selective excitation and inversion along the ^{13}C channel.

3. Results and discussion

3.1. Pulse sequence and magnetization transfer in hncoCANH and hnCOcaNH experiments

The pulse sequences for hncoCANH and hnCOcaNH experiments are shown in Fig. 1A and B, respectively. They are both derived from the basic sequence of HN(C)N [11] and differ in the way the t_1 evolution is handled. Therefore, the transfer efficiency functions which dictate the intensities of self and sequential correlation peaks in the hncoCANH and hnCOcaNH spectra would be the same as those of HN(C)N spectra described previously [11]. Thus, we present here only the distinguishing features of both these spectra.

Fig. 2A and B traces the magnetization transfer pathways along with the respective frequency labeling schemes in the two experimental sequences. Both the experiments start with an INEPT transfer of magnetization from the H^N proton of residue *i* to the directly attached ^{15}N spin via the one-bond (90–95 Hz) $^{1}H–^{15}N$ coupling. This is followed by a ^{15}N constant time ($2T_N$) evolution period. During this period the $^{15}N_i$ magnetization evolves under: (a) one-bond (14–15 Hz) $^{15}N–^{13}C'$ coupling and (b) one-bond (90–95 Hz) $^{1}H–^{15}N$ coupling. At the end of this period, $^{15}N_i$ magnetization becomes: (a) in-phase with respect to its amide $^{1}H^N$ proton and (b) anti-phase with respect to the $^{13}C'_{i-1}$. It is then transferred to $^{13}C'_{i-1}$ through a pair of 90° pulses on ^{15}N and $^{13}C'$. It is followed by a period $2\tau_C$ during which one-bond (55 Hz) $^{13}C'–^{13}C^{\alpha}$ coupling evolves. After this point the two experiments differ slightly, especially with regard to t_1 evolution. In the hnCOcaNH experiment the $^{13}C'$ magnetization is frequency-labeled by evolution under chemical shift (t_1) before it evolves under $^{13}C'–^{13}C^{\alpha}$ coupling (see Fig. 1B), whereas in the hncoCANH experiment there is no frequency labeling at this stage. At the end of this period, $^{13}C'_{i-1}$ magnetization is anti-phase with respect to the $^{13}C^{\alpha}_{i-1}$. The magnetization is then transferred to $^{13}C^{\alpha}_{i-1}$ through a pair of 90° pulses on $^{13}C'$ and $^{13}C^{\alpha}$. This is followed by a $^{13}C^{\alpha}$ constant time ($2\tau_{CN}$) evolution period. During this period, the $^{13}C^{\alpha}_{i-1}$ magnetization evolves under: (a) one-bond (7–11 Hz) and two-bond (4–9 Hz) $^{15}N–^{13}C^{\alpha}$ coupling and (b) one-bond (55 Hz) $^{13}C'–^{13}C^{\alpha}$ coupling. Now, in the case of hncoCANH experiment, the $^{13}C^{\alpha}_{i-1}$ magnetization is frequency-labeled by evolution under chemical shift (t_1) during this constant time period. At the end of this period, $^{13}C^{\alpha}_{i-1}$ magnetization becomes: (a) in-phase with respect to its $^{13}C'$ and (b) anti-phase with respect to the $^{15}N_i$ and $^{15}N_{i-1}$ magnetization. It is then transferred to the respective $^{15}N_i$ and $^{15}N_{i-1}$ nuclei by a pair of 90° pulses on $^{13}C^{\alpha}$ and ^{15}N. This is followed by another ^{15}N constant time ($2\tau_N$) evolution period including t_2. During this period, the ^{15}N magnetization evolves under: (a) one-bond (7–11 Hz) and two-bond (4–9 Hz) $^{15}N–^{13}C^{\alpha}$ coupling and (b) one-bond (90–95 Hz) $^{1}H–^{15}N$ coupling. At the end of this period, the ^{15}N magnetization becomes: (a) in-phase with respect to $^{13}C^{\alpha}$ and (b) anti-phase with respect to its amide proton. Finally, the ^{15}N magnetization is transferred back to the amide proton for detection.

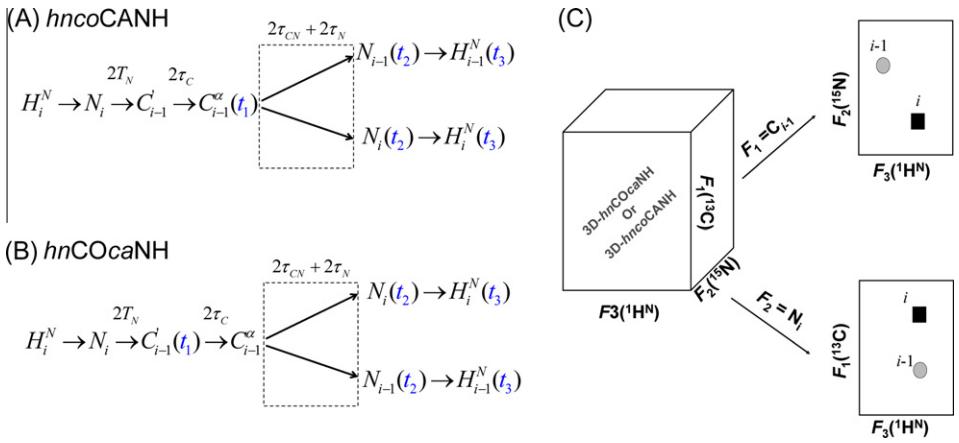

Fig. 2. (A) and (B) Schematic diagram showing the magnetization transfer pathway and frequency labeling in the hncoCANH and hnCOcaNH experiments. T_N, τ_C, τ_{CN}, and τ_N are the delays during which the transfers indicated by the arrows take place in the pulse sequences, (C) schematic three-dimensional spectrum and the correlations observed in the F_1–F_3 and F_2–F_3 planes, respectively, at the ^{13}C chemical shift of residue $i-1$ and ^{15}N chemical shift of residue i. Squares and circles represent the self and sequential peaks, respectively. Black and gray represent positive and negative signs, respectively.

3.2. Amino acid sequence-dependent peak patterns in the hncoCANH and hnCOcaNH spectra

As shown schematically in Fig. 2C, the peaks appear at the following coordinates in the 3D spectrum of hncoCANH and hnCOcaNH:

$$F_1 = C_{i-1}, (F_3, F_2) = (H_i, N_i), (H_{i-1}, N_{i-1})$$
$$F_2 = N_i, (F_3, F_1) = (H_i, C_i), (H_i, C_{i-1})$$

The letter "C" here refers to $^{13}C^{\alpha}$ and $^{13}C'$ chemical shifts, respectively, in hncoCANH and hnCOcaNH spectra. Thus, the F_2–F_3 plane corresponding to $F_1 = C_{i-1}$, shows a self peak (H_i, N_i) and a sequential peak (H_{i-1}, N_{i-1}) to residue, $i-1$ and the F_1–F_3 plane corresponding to $F_2 = N_i$, shows a self peak (H_i, C_i) and a sequential peak (H_i, C_{i-1}) to residue, $i-1$.

As in the case of the HN(C)N experiment the self and sequential peaks have opposite signs except in special situations. Considering different triplets of residues, covering the general and all the special situations, the expected peak patterns in different planes of the hncoCANH and hnCOcaNH spectra have been shown in Fig. 3 where squares and circles represent self and sequential peaks, respectively. Fig. 3A shows the expected peak patterns in the F_2–F_3 planes of the hncoCANH/hnCOcaNH spectrum at the $F_1(^{13}C)$ chemical shift of residue, illustrated using an arbitrary sequence –PXGYZP–. The black circle/square peak is taken to be positive,

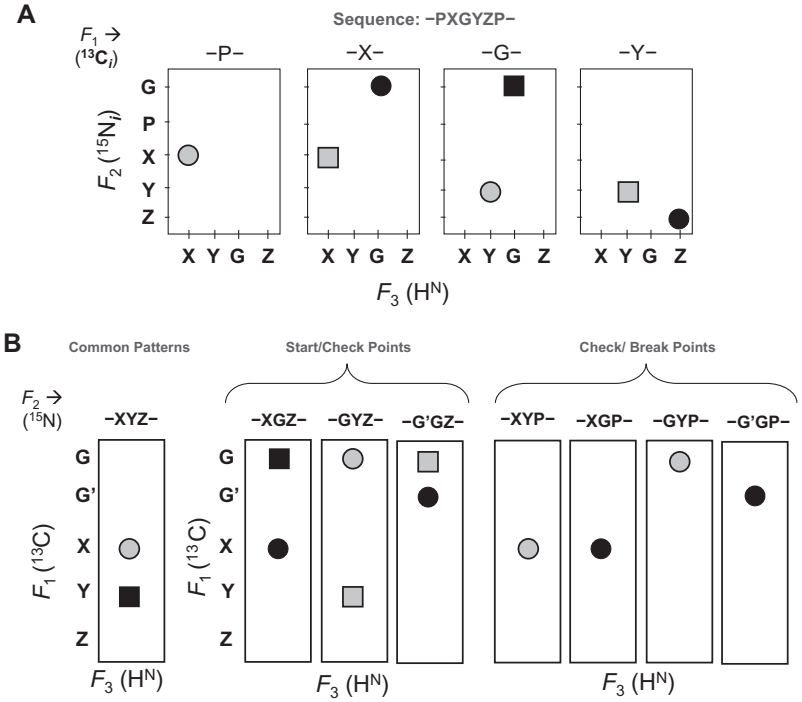

Fig. 3. (A) Schematic peak patterns in the F_2–F_3 planes of the hncoCANH and hnCOcaNH. An arbitrary amino acid sequence is chosen to illustrate the triplet specific peak patterns in these planes of the spectra and (B) schematic peak patterns in the F_1–F_3 planes of the hncoCANH and hnCOcaNH and the corresponding triplet of residues. Black and Gray colors represent positive and negative signs, respectively. Squares and circles represent the self and sequential peaks, respectively. X, Y and Z are any residues other than glycine and proline. G and P represent glycine and proline, respectively. The patterns involving G serve as start and/or check points during a sequential assignment walk through the spectrum. The patterns involving P identify break points during a sequential walk.

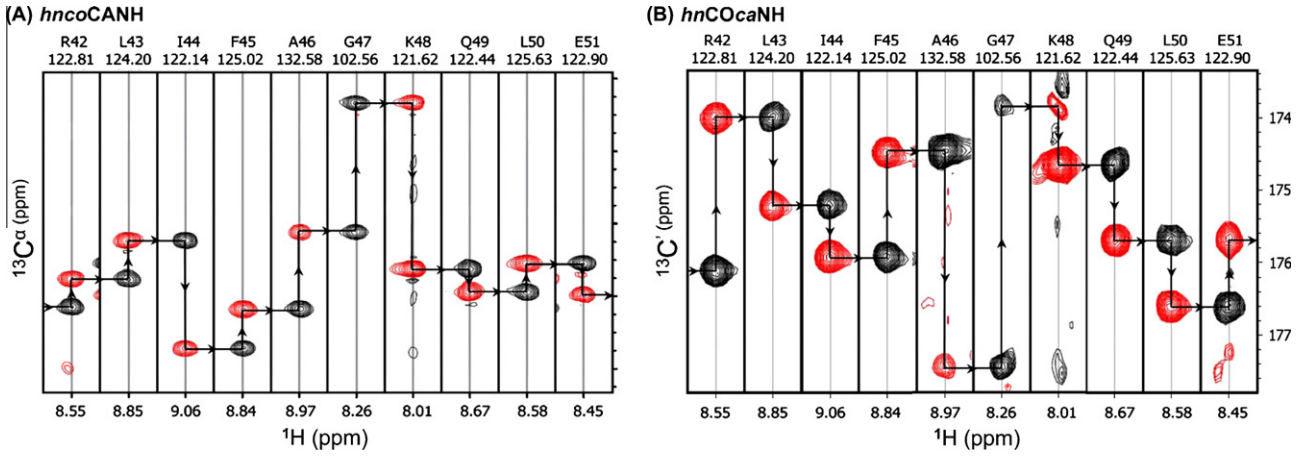

Fig. 4. (A) The illustrative stretches of sequential walk (for residues Arg42-Glu51 in ubiquitin) through $F_1(^{13}C')$–$F_3(^1H)$ planes of the hncoCANH (A) and 3D-hnCOcaNH (B) spectra. The red and black contours indicate positive and negative peaks, respectively. A horizontal line connects a self peak (red) in one plane to a sequential peak (black) in the adjacent plane on the right, except at the check points where the signs will be different. Note that the panels of G47 and K48 constitute the check points in this sequential walk. The numbers at the top in each panel in A and B identify the $F_2(^{15}N)$ chemical shifts, which help identification of the self peaks. (For interpretation of the references to colour in this figure legend, the reader is referred to the web version of this article.)

and the grey circle/square is taken to represent a negative peak. The actual signs in the spectrum are dictated by whether the $i-1$ residue is a glycine or otherwise, and of course by the phasing of the spectra. Here, we have made the self negative for a central residue of a triplet sequence when glycine is at the $i-1$ position. From the figure, it is clear that glycines make an important difference in the expected patterns of peaks, as also the prolines, which do not have an amide proton; hence there is no corresponding peak.

Fig. 3B shows the expected peak patterns in the F_1–F_3 planes of the hncoCANH/hnCOcaNH spectra for several triplets of residues at the $F_2(^{15}N)$ chemical shift of residue *i*. The signs of peaks *i* and $i-1$ in this plane are dictated by the nature of the residues at positions *i* and $i-1$, respectively. In Fig. 3B, each panel represents the F_1–F_3 plane at the ^{15}N chemical shift (F_2) of the central residue in the triplet. For glycines, the evolutions of the magnetization components are slightly different because of the absence of the β-carbon. This in turn generates some special patterns depending on whether the *i*th or $(i-1)$th residue is a glycine or otherwise (Fig. 3B, middle and last panels). These special peak patterns – which help in the identification of glycines and the residues present next to the glycines in triplet sequences – provide important start or check points during the course of sequential assignment process. Further, the absence of amide proton for prolines, at position $i+1$ in the triplet stretches, results in the absence of the self peak (H_i, C_i). This will generate other types of special patterns depending on whether the $(i+1)$th residue is a proline or otherwise (Fig. 3B, last panel). These special peak patterns – which help in the identification of residues preceeding the prolines in the triplet sequences – provide stop or break points during the course of the sequential assignment walk. This facilitates the assignment process further. The important points to remember are: (i) the sign of the self peak for a residue following a glycine is always opposite to that of any other residue and (ii) the signs of the self (i) and sequential ($i-1$) peaks in a particular F_1–F_3 plane of the spectra are same for glycines and the residues following glycines, though the signs are opposite in the two cases. For example, in a stretch XGZ, in the F_1–F_3 plane at the ^{15}N chemical shift of G, the ^{13}C peaks of G and X will have the same sign (negative) and likewise, in the F_1–F_3 plane at the ^{15}N chemical shift of Z, the ^{13}C peaks of Z and G will also have the same but opposite sign (i.e. positive). Thus, for a given protein with a known amino acid sequence, it is possible to identify several special triplet sequences simply by inspecting the various F_1–F_3 planes in the hncoCANH and hnCOcaNH spectra of the protein. Note that in all these peak patterns the glycine ^{13}C chemical shift is taken to be distinctly upfield compared to that of the other residues. This is true in case of hncoCANH spectrum where $^{13}C^{\alpha}$ chemical shifts of glycines are most up-field shifted (~43–50 ppm) compared to other amino acids. However, in case of hnCOcaNH spectrum, where glycine residues cannot be identified by their $^{13}C'$ chemical shifts, the sign inversion might lead to some confusion since the distinction between self and sequential peaks is based on the signs of peaks. But, this can be sorted out when used in conjunction with the hncoCANH experiment. These features of the two spectra have been tested and demonstrated with 1.6 mM ubiquitin (76 aa). Fig. 4 shows the F_1–F_3 planes from hncoCANH (A) and hnCOcaNH (B).

3.3. Assignment protocol

The assignment strategy proposed here is a consequence of: (a) sequential ^{15}N and ^{13}C correlations ($i \rightarrow i-1$) and (b) the distinctive peak patterns of self and sequential peaks in different planes of the hncoCANH and hnCOcaNH spectra which enable ready identification of certain specific triplet sequences (Fig. 3). The hncoCANH provide correlation between amide resonances of one residue (i) to the $^{13}C^{\alpha}$ carbon resonances of the same residue (i) and the previous residue ($i-1$), while the hnCOcaNH provides correlation between amide resonances of one residue (i) to the $^{13}C'$ carbon resonances of the same residue (i) and the previous residue ($i-1$). In cases, when the $^{13}C^{\alpha}$ chemical shifts of i and $i-1$ residues are degenerate in hncoCANH spectrum, the hnCOcaNH spectrum would be useful and vice versa. The assignment protocol based on these spectra is very simple and straight forward. First, find the sequential connectivities between the HSQC peaks using the sequential ^{13}C correlations and then use the check point information derived from triplet specific peak patterns (Fig. 3) to code this information into a format like –XXXGBXGBXP–. Here X is any HSQC peak giving common peak pattern (Fig. 3) and G is the HSQC peak identified as glycine from triplet specific peak patterns (Fig. 3) and B is the HSQC peak identified as residue succeeding a glycine from triplet specific peak patterns (Fig. 3). P here refers to break point identified again from triplet specific peak patterns (Fig. 3). Now compare the above written sequence (i.e. –XXXGBXGBXP–) with the primary sequence of the protein to find a match. Thus, the single experiment provides direction specific

sequential walk and no complementary experiment is required. The main advantage of the present protocol as compared to the currently used protocols based on triple resonance experiments HNCA/HN(CO)CA, HN(CA)CO/HNCO, and CBCANH/CBCA(CO)NH, etc. is that because of the large number of check points that are generally available, explicit side chain assignment would not be very necessary to decide on the correctness of the sequential assignment.

There is another important difference in the assignment strategy presented here compared to that based on HNCA or HN(CA)CO where one has to scan the nitrogen planes to find the matching carbon peaks, which may lead to ambiguities. In the present case there is no need for any repeated scanning through the planes since the carbon planes would directly provide the positions of N_i and N_{i-1} (Figs. 2A and 3A). More explicitly, start with an HSQC peak *i*. The ^{15}N plane for this in hncoCANH/hnCOcaNH spectra would provide the C_i and C_{i-1} positions. The C_{i-1} plane of the same spectrum would provide the N_i (already known) and N_{i-1} positions along with the amide positions as in the HSQC spectrum.

Further, at times when self and sequential correlation peaks are very close to each other and if they are of the same sign – as is the case in the standard HNCA and CBCANH experiments – both the peaks appear as one and then the distinction between them becomes difficult. However, in case of hncoCANH and hnCOcaNH spectra, the positive and negative signs make this condition less possible and results in a dispersive peak shape which in turn indicates that the self and sequential peaks are lying close to each other. However, cancellation of intensities can occur whenever two neighboring residues (i and $i-1$) have almost identical ^{13}C chemical shifts.

Both the experiments have been successfully tested on $^{13}C/^{15}N$ labeled 1.6 mM ubiquitin. In both the experiments, complete sequential connectivities were seen. The complete sequential walks through these spectra have been shown in Supplementary material (Fig. S1 for hncoCANH and Fig. S2 for hnCOcaNH). We believe that these experiments will be of great value for high-throughput NMR structural studies of proteins.

4. Conclusion

In conclusion two triple resonance pulse sequences – named as hncoCANH and hnCOcaNH – have been described here which can provide complete backbone assignment of $^1H^N$, ^{15}N, $^{13}C^\alpha$, and $^{13}C'$ resonances in isotopically enriched proteins. Each experiment correlates the ^{15}N and $^1H^N$ chemical shift of a protein residue (i) to the intra-residue (i) and inter-residue ($i-1$) carbon resonance ($^{13}C^\alpha$ and $^{13}C'$, respectively, in *hnco*CANH and *hn*CO*ca*NH). The main strength of the experiments proposed here is that the self and the sequential correlations appear opposite in-phase and hence can easily be identified without using any other complementary experiment which in general is the case with most other NMR experiments routinely used for the same purpose (like (a) HNCACB [3] and CBCANH [2] in conjunction with CBCACONH [7], (b) HN(CA)CO [6] in conjunction with HNCO [4,5] or intra-HN(CA)CO [10] and (c) HNCA [4,5] in conjunction with HN(CO)CA [4] or sequential HNCA [8] or intra-HNCA [9]). Hence the present experiments would help reduce the data acquisition time and speed up the assignment process.

Finally, a few comments on the sensitivity of the experiments are also required to be mentioned here. This is important since the experiment employs many steps of magnetization transfer and there could be loss of signal through the pulse sequence. While this is not a serious problem in small proteins and denatured/unfolded proteins, it may become a matter of concern for larger folded proteins which have fast relaxation rates. The sensitivity problem can be circumvented by incorporation of the TROSY option [14] in the pulse sequences along with per-deuteration of the proteins to reduce relaxation losses. Overall the hnCOcaNH spectrum has a slightly lower sensitivity compared to hncoCANH, as in the former, $^{13}C'$ chemical shift is evolved in a real time manner. Even so, the results presented here indicate that the experiments are still practical and reasonable sensitivities are evident. Further, at the currently available higher magnetic fields, the sensitivities will be much higher. Thus, sensitivity of the hncoCANH and hnCOcaNH techniques is not as much of an issue and experiments can be successfully carried out on large proteins. Thus, we believe that the pulse sequences described here will be of very general use in all structural-genomics efforts.

Acknowledgment

We thank Government of India for providing financial support to the National Facility for High Field NMR at Tata Institute of Fundamental Research, India.

Appendix A. Supplementary material

Supplementary data associated with this article can be found, in the online version, at doi:10.1016/j.jmr.2010.06.013.

Reference

[1] P. Permi, A. Annila, Coherence transfer in proteins, Prog. Nucl. Magn. Reson. Spectros. 44 (2003) 97–137.
[2] S. Grzesiek, A. Bax, An efficient experiment for sequential backbone assignment of medium-sized isotopically enriched proteins, J. Magn. Reson. B 99 (1992) 201–207.
[3] M. Wittekind, L. Mueller, HNCACB, a high-sensitivity 3D NMR experiment to correlate amide-proton and nitrogen resonances with the alpha- and beta-carbon resonances in proteins, J. Magn. Reson. B 101 (1993) 201–205.
[4] S. Grzesiek, A. Bax, Improved 3D triple-resonance NMR techniques applied to a 31 kDa protein, J. Magn. Reson. A 96 (1992) 432–440.
[5] L.E. Kay, M. Ikura, R. Tschudin, A. Bax, Three-dimensional triple-resonance NMR spectroscopy of isotopically enriched proteins, J. Magn. Reson. B 89 (1990) 496–514.
[6] R.T. Clubb, V. Thanabal, G. Wagner, A constant-time three-dimensional triple-resonance pulse scheme to correlate intraresidue $^1H^N$, ^{15}N, and ^{13}CO chemical shifts in ^{15}N–^{13}C-labelled proteins, J. Magn. Reson. A 97 (1992) 213–217.
[7] S. Grzesiek, A. Bax, Correlating backbone amide and side chain resonances in larger proteins by multiple relayed triple resonance NMR, J. Am. Chem. Soc. 114 (1992) 6293.
[8] A. Meissner, W. Sørensen, A sequential HNCA NMR pulse sequence for protein backbone assignment, J. Magn. Reson. A 150 (2001) 100–104.
[9] B. Brutscher, Intraresidue HNCA and COHNCA experiments for protein backbone resonance assignment, J. Magn. Reson. 156 (2002) 155–159.
[10] D. Nietlispach, A selective intra-HN(CA)CO experiment for the backbone assignment of deuterated proteins, J. Biomol. NMR 28 (2004) 131–136.
[11] S.C. Panchal, N.S. Bhavesh, R.V. Hosur, Improved 3D triple resonance experiments, HNN and HN(C)N, for HN and ^{15}N sequential correlations in (^{13}C, ^{15}N) labeled proteins: application to unfolded proteins, J. Biomol. NMR 20 (2001) 135–147.
[12] R. Keller, The Computer Aided Resonance Assignment Tutorial CANTINA, Verlag, Goldau, Switzerland, 2004.
[13] L. Emsley, G. Bodenhausen, Gaussian pulse cascades: new analytical functions for rectangular selective inversion and in-phase excitation in NMR, Chem. Phys. Lett. 165 (1990) 469–476.
[14] K. Pervushin, R. Riek, G. Wider, K. Wuthrich, Attenuated T2 relaxation by mutual cancellation of dipole–dipole coupling and chemical shift anisotropy indicates an avenue to NMR structures of very large biological macromolecules in solution, Proc. Natl. Acad. Sci. USA 94 (1997) 12366–12371.
[15] A.J. Shaka, J. Keeler, R. Freeman, Evaluation of a new broadband decoupling sequence: WALTZ-16, J. Magn. Reson. 53 (1983) 313–340.
[16] A.J. Shaka, J. Keeler, T. Frankiel, R. Freeman, An improved sequence for broadband decoupling: WALTZ-16, J. Magn. Reson. 52 (1983) 335–338.
[17] A.J. Shaka, P.B. Barker, R. Freeman, Computer-optimized decoupling scheme for wideband applications and low-level operation, J. Magn. Reson. 64 (1985) 547–552.
[18] D. Marion, M. Ikura, R. Tschudin, A. Bax, Rapid recording of 2D NMR spectra without phase cycling. Application to the study of hydrogen exchange in proteins, J. Magn. Reson. 85 (1989) 393–399.
[19] M. Piotto, V. Saudek, V. Sklenar, Gradient-tailored excitation for single-quantum NMR spectroscopy of aqueous solutions, J. Biomol. NMR 2 (1992) 661–665.